

Exact diagonalization study of the hole distribution in CuO_3 chains within the four-band dp model

S.-L. Drechsler* and J. Málek†

Institut für Festkörper- und Werkstofforschung Dresden e.V., Postfach 270016, D-01171 Dresden, Germany

H. Eschrig

Max-Planck-Arbeitsgruppe "Elektronensysteme" an der Technischen Universität Dresden, D-01169 Dresden, Germany

(Received 12 April 1996; revised manuscript received 8 August 1996)

We consider the hole distribution in CuO_3 chains as a function of the total hole number $0 \leq n \leq 2$ per chain unit within the standard dp model containing one orbital per site. The nonequivalency of the apical and the chain oxygen sites is taken into account explicitly. Using slightly modified standard CuO_2 plane parameter sets, we compare the results of exact diagonalization studies of periodic and open CuO_3 chains with experimental data for $\text{YBa}_2\text{Cu}_3\text{O}_{7-\delta}$ (YBCO) and $\text{Ca}(\text{Sr})_2\text{CuO}_3$, and with theoretical results obtained within the following often used approximations: the Hartree-Fock and the local ansatz approximations, as well as with the exclusion of double occupancies at Cu sites and also that at oxygen ones (spinless fermion picture). We have found out that the ratio of the hole densities on the apical and the chain oxygen sites is sensitive to the magnitude of the nearest-neighbor Coulomb interaction V_{pd} and the difference of their site energies Δ_{pp} . Adopting values $V_{pd} \sim 1$ eV and $V_{pp} \sim 0.5V_{pd}$, we estimate $\Delta_{pp} = 1.5$ to 2.5 eV for YBCO from the comparison with O $1s$ x-ray absorption spectroscopy and ^{17}O nuclear magnetic resonance data. Using experimental values of the corresponding binding energies and the components of the electric field gradient tensor, the site energy of the apical oxygen $2p_z$ states relative to the planar copper $\text{Cu}(2) 3d_{x^2-y^2}$ states is estimated as ~ 5 to 6 eV. With increasing hole doping and/or the strength of V_{pd} , the holes are increasingly localized at the apical oxygen sites. Various chain aspects of proposed scenarios for the $\text{PrBa}_2\text{Cu}_3\text{O}_7$ problem are briefly discussed. [S0163-1829(96)04546-8]

I. INTRODUCTION

There is an increasing interest in the electronic structure of CuO_3 chains which occur in various cuprates.¹⁻⁹ In the $R\text{Ba}_2\text{Cu}_3\text{O}_{7-\delta}$ compounds ($R = \text{Y, La, rare earth; } \delta \approx 0.0$ to 0.5), these chains control the doping of the CuO_2 planes and thereby also the plane-dominated superconductivity, whereby the exact relation of the mobile hole concentrations within chains and planes as well as the origin of the superconducting condensate observed experimentally in the chains, too, is still unclear.¹⁰⁻¹³ Notably, a simple plane-induced chain superconductivity due to the usual proximity effect has been excluded in Ref. 10.¹⁴

In addition to the knowledge of the total hole content per chain unit, a quantitative understanding of the hole distribution among the apical and chain oxygen sites of CuO_3 chains might also shed light on the applicability of nonstandard microscopic scenarios to describe the chain superconductivity,¹⁵ as well as the magnetic, electronic, and chain-related lattice instabilities¹⁶⁻¹⁸ as suggested on the basis of recent experimental observations.²⁻⁵

The physics of the charge transfer between chains and planes depends crucially on the properties of the apical oxygens which themselves form an important part of the chains. In this context we mention quite interesting phenomena ascribed in the literature to the apical oxygen anharmonicity,¹⁹ as well as the controversial discussion on the topic as to how the apical oxygens affect the superconducting pairing mechanism within the planes.²⁰ In particular, the site energy of the

apical oxygen $2p_z$ states is of prime interest within the context of multi band models for the occupation of the plane-copper $3d_{z^2}$ orbital in competition with that of the plane Zhang-Rice singlet states.²⁰⁻²³

A detailed knowledge of the charge distribution on the chains is also necessary for the assessment of hypotheses involving hole doping of the chains²⁴ or of the Ba-O(4) planes²⁵ in order to explain the absence of superconductivity and metallicity in the anomalous $\text{PrBa}_2\text{Cu}_3\text{O}_7$ compound.

Finally, the interpretation of recent data responding to optics,²⁶ magnetic susceptibility,²⁷⁻³⁰ and transport³¹⁻³³ of the linear chain cuprates $(\text{Ca,Sr})_2\text{CuO}_3$ requires theoretical investigations of CuO_3 chains within realistic microscopical models.³⁴

We regard the standard dp model with one orbital per site as a reasonable starting point to discuss some chain-related aspects of the above-mentioned problems quantitatively. A first step in this direction was taken by Oleś and Grzelka,³⁵ who studied the hole distribution in CuO_3 chains within the dp four-band approach applying the Hartree-Fock approximation (HFA) and the local ansatz (LA) technique. Following these lines, in the present paper we shall compare the predictions of Ref. 35 and some other often-used approximation in the cuprate literature with the results obtained by the exact diagonalization technique for small clusters. In addition, we shall investigate the consequences of a possible (large) difference of apical and chain oxygen site energies Δ_{pp} as suggested in Refs. 7, 20, and 36 and the effect of Coulomb interaction between oxygen sites $V_{pp} \sim 0.5V_{pd}$

which have not been studied in Ref. 35.

There is a large body of (chainlike) cluster calculations in the literature. Here, we refer only to the recent works of Aligia *et al.*⁷ and to the *ab initio* study of Mei and Stollhoff.³⁷ The former map the low-energy peaks of the optical conductivity, $\sigma(\omega)$, resulting from the four-band *dp* model as considered here (but with different parameters than ours) onto the *t*-*J* model in order to evaluate $\sigma(\omega)$ for long chains in the ir frequency region.

In the latter work for clusters of the same size as in our calculations, the effect of an extended basis (including Cu $3d_{z^2}$ as well $4s$ and $4p$ orbitals), the averaged charge densities, and the spin-correlation function have been studied within the local ansatz approximation.

In the present paper we shall address mainly three problems: (i) how the hole distribution changes as a function of the total hole content per unit cell, (ii) how several popular *dp*-parameter sets proposed for the layered cuprates³⁸⁻⁴¹ should be modified for the cuprate chains in order to describe available experimental data, and, finally, (iii) how important correlation effects are for the electronic structure of CuO_3 chains in various materials.

The paper is organized as follows. In Sec. II we discuss the total hole content per CuO_3 chain unit for various chain-bearing materials. Some remarks on the choice of the *dp*-model parameters and the calculated quantities are made in Sec. III. The results of our study are presented in Sec. IV. The accuracy of the Hartree-Fock approximation (HFA) and the local ansatz (LA) and the double occupancy exclusion (DOE) approximations with respect to the hole distribution are discussed in Sec. IV A. The general trends of the hole distribution among the nonequivalent sites n_i , $i=1-3$, as a function of the total hole content n per chain unit and for fixed $n=1.5$ (corresponding approximately to $\text{YBa}_2\text{Cu}_3\text{O}_7$) as a function of the model parameters are considered in Sec. IV B. In Sec. IV C we present our results for the spin-spin correlation function and compare them with the *ab initio* cluster calculations of Mei and Stollhoff.³⁷ Following that, a short discussion of the interpretation of the O $1s$ x-ray absorption spectroscopy (XAS) transition energies and Madelung energies in terms of oxygen site energies in the *dp* model is given in Sec. IV D. Possible consequences for chain aspects of various scenarios proposed to explain the absence of superconductivity and metallicity of the $\text{PrBa}_2\text{Cu}_3\text{O}_7$ compound are briefly discussed in Sec. IV E. Possible long-range ordered states for half- and quarter-filled chains are briefly discussed in Sec. IV F. We end with Sec. V, where conclusions are drawn and prospects for further theoretical and experimental studies are discussed.

II. OXIDATION STATE AND HOLE COUNT OF CuO_3 CHAINS

Layered cuprate structures contain three types of anionic cuprate complexes: extended CuO_2 planes, extended CuO_3 chains, and isolated CuO_2 dumbbells (see Fig. 1). While the isolated dumbbells appear exclusively in the $(\text{CuO}_2)^{-3}$ oxidation state (monovalent Cu), planes and chains are subject to mutual doping.

Known structures containing CuO_3 chains are $R\text{Ba}_2\text{Cu}_3\text{O}_{7-\delta}$ ($0 \leq \delta < 1$) with *R* being Y, La, or any rare-

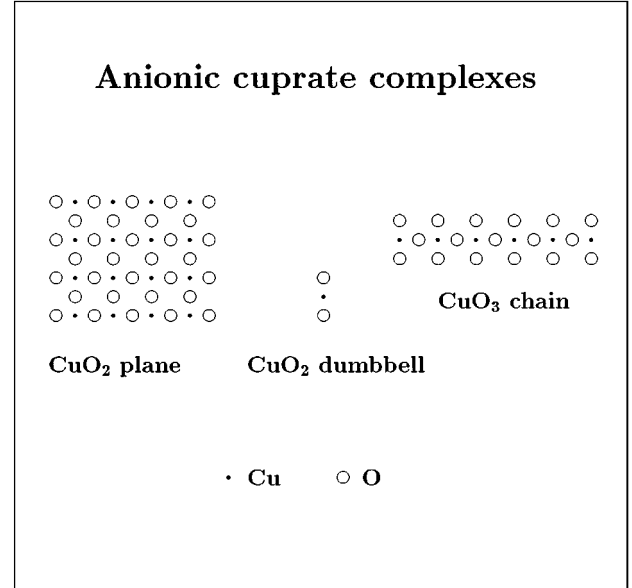


FIG. 1. Anionic cuprate complexes in typical layer structures considered in the present paper: CuO_2 plane (left), CuO_2 dumbbell (middle), and CuO_3 chain (right).

earth element, $(\text{Sr}, \text{Ca})_2\text{CuO}_3$,^{28,27} and $(\text{Sr}, \text{Ca})_{2-x}\text{Na}_x\text{CuO}_3$ ($x \leq 0.5$).^{31,32} The cationic oxidation states are $(R\text{Ba}_2)^{7+z}$, $(\text{Sr}, \text{Ca})_2^{+4}$, and $(\text{Ca}_{2-x}\text{Na}_x)^{+4-x}$, respectively. Hence the oxidation state of the chain complex of the latter two materials is well determined to be $(\text{CuO}_3)^{-4}$ in $(\text{Sr}, \text{Ca})_2\text{CuO}_3$ and $(\text{CuO}_3)^{-4+x}$ in $\text{Ca}_{2-x}\text{Na}_x\text{CuO}_3$. Recently, $\text{Sr}_2\text{CuO}_{3+\delta}$ with excess oxygen was reported³³ for which the oxidation state of the chain complex would also be $(\text{CuO}_3)^{-4+x}$, $x=2\delta$ provided homogeneous doping has been achieved.

The situation with $R\text{Ba}_2\text{Cu}_3\text{O}_{7-\delta}$ is much more involved, because in this structure all three anionic cuprate complexes are present, and, moreover, some cations may not be fully ionized, causing $z < 0$ (Ref. 25) or tending to a higher valency, causing $z > 0$. Obviously, the ‘‘alloy’’ cases of $R_{1-z}M_z\text{Ba}_2\text{Cu}_3\text{O}_{7-\delta}$ and $R\text{Ba}_{2-z}Q_z\text{Cu}_3\text{O}_{7+\delta}$, where nontrivalent ions $M=\text{Ca}, \text{Th},$ or Ce occupy the *R* site,⁴² or when trivalent ions $Q=\text{La}(\text{Nd})$ occupy the Ba site and some additional oxygen ions ($\delta \sim 0.07$) reside on O(5) sites,^{43,44} can be included in the consideration of the two former clean cases. The oxidation state of the planes is $(\text{CuO}_2)^{-2+y}$, where y is the deviation from half-filling of the uppermost antibonding *d*-*p* band. Its value depends on the constitution of the material. There are always two planar CuO_2 complexes per formula unit. In the most ordered case, with $\delta=j/(j+k)$ being a rational number (j, k small integers), there are j perfect chains alternating with k rows of dumbbells. Hence, there are $(1-\delta)$ chain complexes per formula unit and δ isolated chain dumbbells $(\text{CuO}_2)^{-3}$. The oxidation state $(\text{CuO}_3)^{-4+x}$ of the chain complex is obtained by summing over all oxidation numbers multiplied by their occurrence number: $(-4+x)(1-\delta)-3\delta+2(-2+y)+(7+z)=0$. One then finds

$$x = 1 - \frac{2y+z}{1-\delta}. \quad (1)$$

Notice that inserting $\delta=0,1/2$ and $z=0$ into Eq. (1) one reproduces the results of Zaanen *et al.*⁴⁵ Disorder of the chain leads to an increasing number of chain ends, ineffective in the intrinsic doping balance: Chain ends behave much like isolated CuO_2 dumbbells. At a given fixed δ , disorder thus leads to a reduction of the number of chain complexes below $(1-\delta)$. Hence, Eq. (1) gives an upper limit for x (since $2y+z$ is always positive for hole doped cuprates) which is expected to be approached from below by careful heat treatment. To illustrate this point, within the simple picture of noninteracting, i.e., randomly distributed vacancies residing at the O(1) site on the CuO_3 chain (compare, e.g., Refs. 46–48), one has

$$\begin{aligned} 2y+z &= 1-x-(2-x)\delta_v+(2+x)\delta_v^2-x\delta_v^3 \\ &\approx 1-x-(2-x)\delta_v, \end{aligned} \quad (2)$$

where $\delta_v \ll 1$ denotes the vacancy concentration.

In most cases, z can be assumed to be zero or negligibly small. For $\delta \approx 0$ (ortho-I structure), one usually finds $y \approx 0.25$ and hence $x \approx 0.5$.⁴⁹ The exception might be $R=\text{Pr}$, where some authors^{50,7} favor similar values $x \approx 0.5$, while others^{51–53} find indications for reduced x and/or y values, or even suggest $y, z \approx 0$ (Ref. 24) and hence $x \approx 1$.

In cases where the hole doping level y of the superconducting, CuO_2 planes of the reduced structures has not been determined experimentally, we estimated it from the empirical relation for the transition temperature to superconductivity^{54,55}

$$\frac{T_c}{T_{c,\max}} = 1 - A \left(\frac{y}{y_{\max}} - 1 \right)^2, \quad (3)$$

with $A \approx 2.1$, $T_{c,\max} \approx 94$ K, and $y_{\max} \approx 0.21$.

For the ortho-II structure with $\delta \approx 0.5$, which is expected to be totally ordered in the thermodynamically stable state, having a transition temperature $T_c \approx 60$ K, one would find, from Eq. (3), $y \approx 0.13$. Similar reduced values $0.14 \leq y \leq 0.2$ have been suggested in the literature.^{1,56,57} This leads to $x \approx 0.5$. Very recently, for $\delta=0.23$, the observation of an ortho-III phase has been reported⁵⁸ with a transition temperature of $T_c \approx 84$ K. It is considered to consist of an ordered structure with two perfect CuO_3 chains alternating with one row of dumbbells. The analysis using Eq. (3) would yield $y \approx 0.16$ and again $x \approx 0.5$. Finally, we speculate that superconductivity observed for $\text{YBa}_2\text{Cu}_3\text{O}_{6.41}$ below $T_c \leq 20$ K is due to the ortho-III structure³⁶ with chains and rows of dumbbells of the ortho-III structure interchanged (hence $\delta=2/3$ in the pure structure). Our analysis via Eqs. (1) and (3) yields $y \approx 0.08$ and once more $x \approx 0.5$ in this case. Related estimates on the basis of the XAS data are discussed in Sec. IV.

Summarizing, we find $x=0$ for $(\text{Sr,Ca})_2\text{CuO}_3$, $0 \leq x < 0.5$ for $\text{Sr}_{2-z}\text{Na}_z\text{CuO}_3$, $0 < x < 0.2$ for $\text{Sr}_2\text{CuO}_{3+\delta}$, and quite stable $x \sim 0.5$ for all superconducting members of the $R\text{Ba}_2\text{Cu}_3\text{O}_{7-\delta}$ family independent of δ , and not discussed here in detail in ‘‘alloy’’ cases also independent of the cationic site where the substitution for ions with higher or lower valency occurs. Thereby in the case of $\text{YBa}_{0.5}\text{La}_{0.5}\text{CuO}_3\text{O}_{7+\delta}$ a reasonably small excess oxygen concentration $\delta \approx 0.087$ has been assumed.

Only for nonsuperconducting compounds must the possibility of significantly different x values again independent of δ also be considered, that is, for $\text{PrBa}_2\text{Cu}_3\text{O}_{7-\delta}$, $x \approx 1$,⁵⁹ and for $\text{YBaLaCuO}_3\text{O}_{7+\delta}$, $x \approx 0$.

A CuO_3 complex with completely filled copper-3d states (Cu-I ion) and completely filled oxygen-2p states would be in an oxidation state $(\text{CuO}_3)^{-5}$. Hence, the total hole number per chain complex in the d - p -band complexes of the chain is

$$n = 1 + x, \quad (4)$$

with x taken from the above analysis. Unfortunately, it is very difficult to determine within a few percent of error experimentally the absolute amount of the hole numbers in the plane and chain subsystems separately.⁵⁵

In any case, it is a timely problem to study the properties of cuprate chains in the range of total hole numbers $1 \leq n \leq 2$, and we are now considering this task.

III. MODEL

We adopt the extended Hubbard model which in the cuprate literature is very often denoted as a multiband dp Hamiltonian. Hence, it is presumed that each site bears one orbital only, namely, the $2p_z$ states of the apical oxygens O(4), the $2p_y$ states of the chain oxygens O(1), and finally the $3d_{z^2-y^2}$ states of the chain coppers Cu(1), where $y(b)$ denotes the chain direction. The dp Hamiltonian reads as

$$\begin{aligned} H = & \sum_i \varepsilon_i \hat{n}_i + \sum_{\langle i,j \rangle, s} t_{ij} (c_{i,s}^\dagger c_{j,s} + \text{H.c.}) \\ & + \sum_i U_{ii} \hat{n}_{i,\uparrow} \hat{n}_{i,\downarrow} + \sum_{\langle i,j \rangle} V_{ij} \hat{n}_i \hat{n}_j, \end{aligned} \quad (5)$$

where $c_{i,s}^\dagger$ creates a hole with spin projection $\pm 1/2$ at site i , $\hat{n}_{i,s} = c_{i,s}^\dagger c_{i,s}$ denotes the number operator, and $\hat{n}_i = \sum_s c_{i,s}^\dagger c_{i,s}$. In the present hole picture the vacuum state of the Hamiltonian, Eq. (5), is given by the Cu $3d^{10}$ O $2p^6$ configuration. For the transfer integrals we use the same sign convention as in Ref. 60. A schematical view of the Madelung (crystal) field effect on the oxygen site energies and the notation of site energy differences are shown in Fig. 2.

Unfortunately, to our knowledge there is no reliable chain parametrization like that for the CuO_2 planes of La_2CuO_4 (Refs. 38–41) for any material containing CuO_3 chains. In these circumstances it is reasonable to start from one of the plane sets. In the present paper we shall refer to two most frequently used plane sets, namely, the set proposed by Hybertsen *et al.*,³⁸

$$U_d = 10.5, \quad U_p = 4, \quad V_{pd} = 1.2, \quad t_{pd} = 1.3,$$

$$t_{pp} = 0.65, \quad \Delta_{pd} = 3.6, \text{ set (I),}$$

and the empirical one of Eskes *et al.*,⁴¹

$$U_d = 8.8, \quad U_p = 6, \quad V_{pd} = 1, \quad t_{pd} = 1.3,$$

$$t_{pp} = 0.65, \quad \Delta_{pd} = 3.5, \text{ set (II)}$$

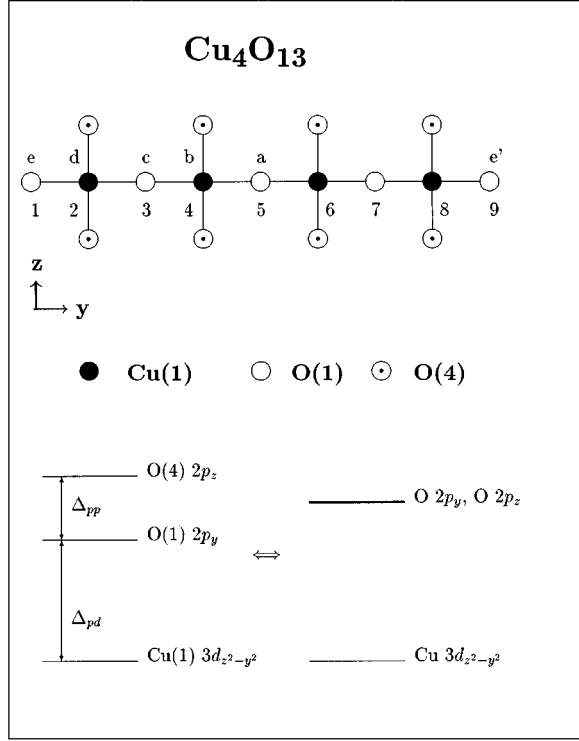


FIG. 2. Upper half: open cluster considered in the present paper. The reference points of the off-diagonal spin-correlation functions shown in Fig. 6 are denoted by a, b, c, d, and e. In the case of periodic boundary conditions for $(\text{CuO}_3)_N$ clusters the sites e and e' coincide. The numbers 1 – 9 denote the site count used in Fig. 6. Lower half: schematic view of the site energies and the crystal field effect on the nonequivalent oxygen sites [apical oxygen O(4) and chain oxygen O(1)].

[all energies are given in eV; cf. the text after Eq. (10) below for the modification of the t_{pd} in the $\text{YBa}_2\text{Cu}_3\text{O}_7$ case].

For the CuO_3 chains the difference of the apical and chain oxygen site energies, $\Delta_{pp} = \varepsilon_{p,a} - \varepsilon_{p,\text{ch}}$, will be treated as a free parameter, whereas for the difference of the Cu(1) and chain oxygen O(1) site energies, $\Delta_{pd} = \varepsilon_{p,\text{ch}} - \varepsilon_d$, a plane value in the charge transfer (CT) limit $U_d, U_p \gg \Delta_{pd} \gg t_{pd}$ is adopted ($\Delta_{pd} \approx 3.5$ eV). The on-site Coulomb interaction parameters U_p at both nonequivalent oxygen sites are assumed to be equal.

Using the Lanczos-method the Hamiltonian [Eq. (5)] has been diagonalized exactly for finite clusters with periodic boundary conditions in chain direction y and also for clusters with open chain ends. Our analysis aims at a study of long chains in thermodynamic equilibrium structures; finite chains are considered due to numerical limitations only. Therefore, following Aligia and Garcés,³⁶ we adopted for open clusters the simple picture where the site energies of all equivalent places including the end sites coincide energetically in electron representation. The cluster size which can be handled numerically depends crucially on the filling ratio. For one hole per chain unit, simulating the $\text{Sr}(\text{Ca})_2\text{CuO}_3$ compounds, clusters composed of up to $N=6$ chain periods have been investigated. For chains with 1.5 holes per chain unit we are restricted to the study of the case $N=4$. Generally, periodic chains $(\text{CuO}_3)_N$ of that size differ only slightly

from open $(\text{CuO}_2)_N\text{O}_{N+1}$ clusters (with oxygen ions at the ends) but deviate somewhat from the more realistic $(\text{CuO}_2)_N\text{O}_{N-1}$ (copper terminated). Aiming at the behavior of open chains of lengths $N \sim 20$ as relevant in real materials, we believe that for many physical properties periodic chains of the uppermost cluster size $N \sim 4$ to 6 which can still be handled by the Lanczos method give a better description than open chains of that size.

Dealing only with ground state properties of the Hamiltonian [Eq. (5)], we report here on results for three quantities: (i) the site expectation value of the hole density n_i ,

$$n_i = \langle G | \hat{n}_i | G \rangle, \quad (6)$$

(ii) the bond order

$$P_{ij} = \frac{1}{2} \left\langle G \left| \sum_s (c_{i,s}^\dagger c_{j,s} + \text{H.c.}) \right| G \right\rangle, \quad (7)$$

and (iii) the spin-correlation function

$$f_{ij} = \langle G | \vec{S}_i \vec{S}_j | G \rangle = \frac{3}{4} \langle G | (n_{i,\uparrow} - n_{i,\downarrow})(n_{j,\uparrow} - n_{j,\downarrow}) | G \rangle, \quad (8)$$

where $|G\rangle$ denotes the ground state and the last relation holds for any singlet state.

As mentioned above, the hole doping of CuO_3 chains within the dp model was first studied by Oleś and Grzelka.³⁵ They adopted a slightly modified version of parameter set (I) suggested by the structural data of $\text{YBa}_2\text{Cu}_3\text{O}_7$. Owing to the shortened O(4)-Cu(1) distance [$R_{pd}^z \approx 1.83 - 1.855$ Å (Ref. 61)] and to the enlarged Cu(1)-O(1) distance ($R_{pd}^y \approx 1.9412$ Å) compared with the mean Cu-O bond lengths [$R_{pd}(I) \approx 1.89$ Å] in the CuO_2 planes of La_2CuO_4 , they adjusted the transfer integrals t_{pd}^y and t_{pd}^z according to the power law parametrization proposed by Harrison,⁶²

$$\frac{t_{pd}}{t_{pd}(I)} = \left(\frac{R_{pd}}{R_{pd}(I)} \right)^{-3.5}, \quad (9)$$

and similarly also the intersite Coulomb interactions V_{pd}^y and V_{pd}^z

$$\frac{V_{pd}}{V_{pd}(I)} = \left(\frac{R_{pd}}{R_{pd}(I)} \right)^{-1.4}. \quad (10)$$

In Ref. 35, $t_{pd}^y = 1.3$ eV, $t_{pp} = 0.65$ eV, and $R_{pd}^z = 1.85$ Å have been adopted, yielding $t_{pd}^z = 1.535$ eV for $t_{pd}^y = 1.3$ eV; i.e., the increase of R_{pd}^y ongoing from La_2CuO_4 to $\text{YBa}_2\text{Cu}_3\text{O}_7$ was ignored. For comparison we note that, in Refs. 7 and 36, $t_{pd}^z = 1.95$ eV, $t_{pd}^y = 1.5$ eV, and $t_{pp} = 0.6$ eV; i.e., significantly larger nearest-neighbor (NN) transfer integrals have been adopted. Except the case when we compare our results with those of Ref. 35 (Sec. IV A), we shall neglect the weak changes following from Eq. (10) because their effect on the calculated quantities is very small. However, the modifications of the transfer integrals according to Eq. (9) will be taken into account. Thus, for calculations devoted to $\text{YBa}_2\text{Cu}_3\text{O}_7$ and to Sr_2CuO_3 we adopt $t_{pd}^y = 1.2$ eV, $t_{pd}^z = 1.416$ eV, $t_{pp} = 0.6$ eV and $t_{pd}^y = t_{pd}^z = 1.2$ eV, $t_{pp} = 0.6$ eV,³⁴ respectively, modifying slightly both parameter sets (I) and (II).

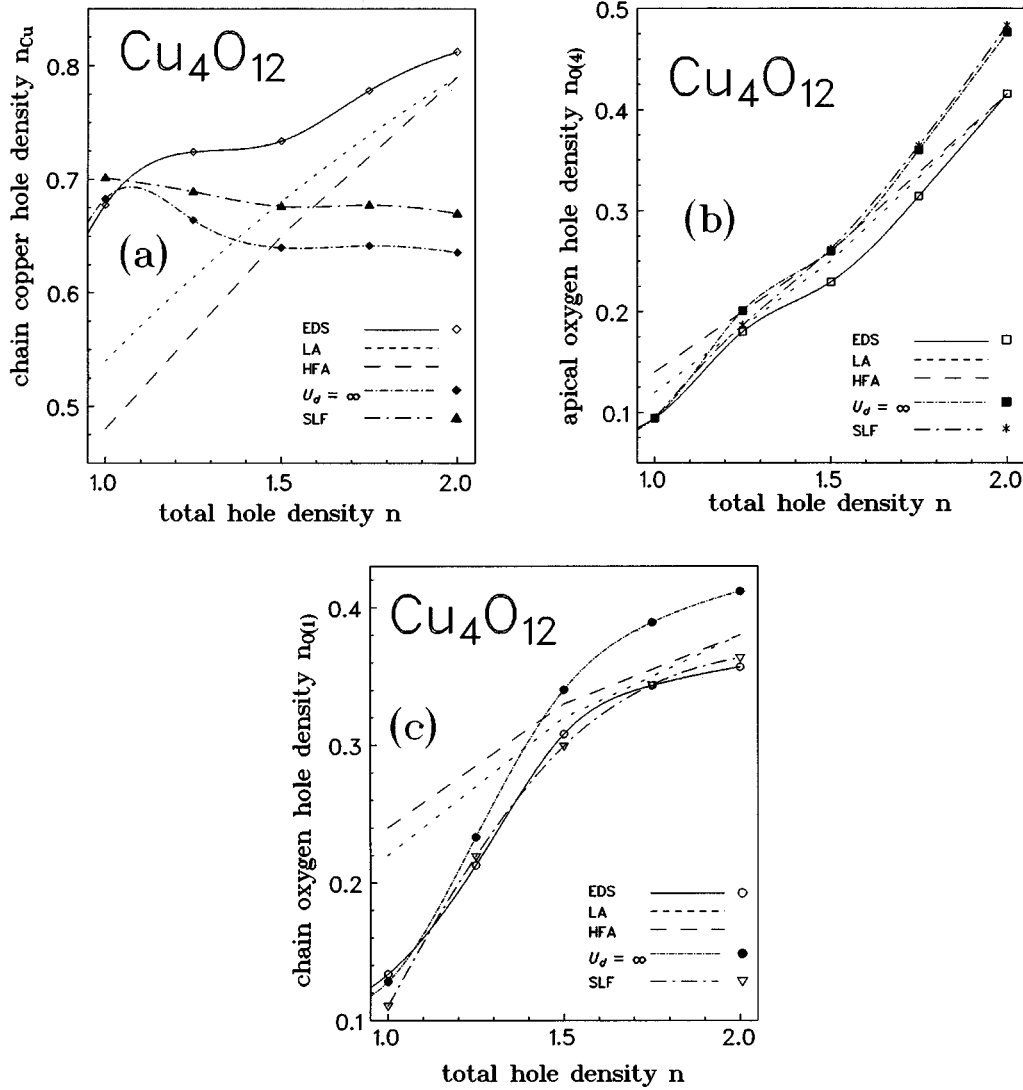


FIG. 3. Hole distribution vs. total hole number n per chain unit for Cu_4O_{12} clusters with periodic boundary conditions evaluated in various techniques: EDS (exact diagonalization), LA (local ansatz, according to Ref. 28), HFA (restricted Hartree-Fock approximation, according to Ref. 28), $U_d \rightarrow \infty$ (exclusion of double occupancy), and spinless fermions (SLF). Chain copper Cu(1) (a), apical oxygen O(4) (b), and chain oxygen O(1) (c). The adopted parameter set includes small modifications compared with the plane set I due to slightly different copper-oxygen distances [see Ref. 28 and Eqs. (9) and (10)].

According to the *ab initio* cluster calculations of Mei and Stollhoff,³⁷ the present Hamiltonian provides a good starting point for the study of the electronic structure of cuprates. Unfortunately, no explicit mapping of their results on the extended Hubbard model has been done. Nevertheless, they recommended not to use a set of interaction parameters in which Δ_{pd} exceeds t_{pd} . In other words, they disregard CT regimes described by parameter sets such as sets (I,II) and favor instead a mixed-valence- (MV-) like interaction regime in the cuprates. In this context it is interesting to compare the charge densities and the spin correlations in CT and MV regimes. With this aim we have performed two calculations for a Cu_4O_{13} cluster bearing four holes taking the Coulomb interaction parameters from set (II) and adopting $\Delta_{pd} = t_{pd}$ and $\Delta_{pd} = 3t_{pd}$ as representative cases for MV and CT interaction regimes, respectively. Since Mei and Stollhoff³⁷ embedded their cluster into a specific ionic environment to neutralize the whole system, we have varied also Δ_{pp} to mimic

the effect of different ionic arrangements because the apical oxygen site energy is sensitive to Madelung field effects.²⁰

IV. RESULTS

A. Comparison of the exact diagonalization with other approaches

Let us begin with the examination of the doping effect (Figs. 3 and 4). In Fig. 3 we compare the hole distribution obtained within the present exact diagonalizational study (EDS) with the results of Oleś and Grzelka³⁵ obtained by the restricted Hartree-Fock approximation (HFA) and the local ansatz (LA) technique. First of all we notice that the general trend of the charge distribution within all three approaches is similar. As expected the largest quantitative deviations between them occur for the case of one hole per chain unit. In this case the LA shifts about 20% of the holes from Cu(1) to

O(1) sites as compared with our EDS results. The results obtained by the HFA exhibit about 25% deviation from the EDS data. We note that the LA predictions are closer to the HFA results rather than to the exact ones. For large hole doping, i.e., $n \approx 2$, only minor deviations between the EDS and the LA as well as even the HFA remain. This is not surprising since at $n=2$ a filled band (closed shell) situation is reached.

Since the size effects for the hole densities n_i and for the total energy per site E_{tot}/N become small for cluster sizes greater than four periods (see Fig. 5), we believe that our EDS results are representative of more extended chains, too. Therefore we ascribe the main differences between the EDS and the LA results to the approximations involved in the LA (e.g., to the usual linearization of the exponential function in the ansatz of the ground state wave function containing the variational parameters) and not to the cluster size.

Finally, we compare our EDS results with the predictions of approaches which exclude double occupations (see, e.g., Refs. 63 and 64). We have simulated the double occupation exclusion (DOE) using large values of $100 < U_d < 500$ eV and taking the limit $U_d \rightarrow \infty$ from our calculations adopting the $1/U_d$ dependence of the charge density. If in addition the limit $U_p \rightarrow \infty$ is taken also, one arrives at the picture of interacting spinless fermions (SLF's).

For weak hole doping $x \ll 1$, i.e., in the vicinity of $n=1$, the DOE approach reveals an almost perfect description. However, for *large* doping ratios $x \geq 0.15$ sizable deviations of the order of 10–20 % occur in comparison with EDS results for realistic finite U_d values ~ 10 eV. Within the SLF the accuracy is somewhat improved (see Fig. 3). In contrast with the LA and HFA for DOE and SLF approaches even the general trend of the hole density at Cu(1) sites becomes wrong for $n \geq 1.25$. Ongoing from $n=1$ to $n=2$ within the EDS, the HFA, and the LA there is a monotonic increase of $n_{\text{Cu}(1)}$ whereas EDO and SLF predict a slight monotonic decrease.

The HFA and LA fail in predicting no ‘‘quasiplateau’’ between $n=1.25$ and $n=1.5$. In general the largest discrepancies have been found for the Cu(1) site followed by the chain oxygen O(1) site.

B. Charge distribution and doping

Let us consider in more detail the doping and the parameter dependences of the charge distribution. Hole doping until 0.5 holes/per CuO_3 unit, i.e., the approximated value expected for $\text{YBa}_2\text{Cu}_3\text{O}_7$, leads to a sizable increase of n_i at both oxygen sites O(4) and O(1) compared with $(\text{Sr,Ca})_2\text{CuO}_3$ ($n=1$). However, a further hypothetical increase of the total hole density almost leads to a saturation at the chain oxygen sites O(1) together with a steep increase at apical oxygen sites O(4). Naturally, this process is affected by the actual value of Δ_{pp} . For example, at $n=2$ for $\Delta_{pp}=0$ the apical oxygen hole density $n_{\text{O}(4)}$ exceeds the chain oxygen one $n_{\text{O}(1)}$ by about 15% [see Figs. 3(b) and 3(c)], whereas at $\Delta_{pp}=1.4$ eV it achieves only 70% of $n_{\text{O}(1)}$ (see Fig. 4). Thus, if the chain is heavily doped with holes $n \rightarrow 2$, the holes should be increasingly located at the apical oxygen sites. The reason for this is the intersite Coulomb repulsion V_{pd} . Indeed, a hole at the O(4) site feels the

repulsion from a second hole at only one Cu(1) neighbor, in contrast to a hole at the chain oxygen site O(1) which has two Cu(1) neighbors.

The general picture of the charge distribution and its evolution with doping obtained for the parameter sets derived from (I) and (II) is very similar. This is not surprising since as mentioned in Sec. III both sets puts the chains into a similar CT-parameter regime. They differ somewhat with respect to the strength of the electron-electron interactions. Comparing Figs. 3 (set I) and 4 (set II) one visualizes that the hole distribution is not very sensitive to the actual strengths of the on-site interactions. In contrast the change of the intersite V_{pd} interaction might yield sizable effects (see below).

Akin to the tendency for $n \rightarrow 2$ to push holes towards the apical oxygens as discussed above, the same physical behavior can be observed already for a lower but fixed hole content. We shall illustrate this for the $n=1.5$ case ($\text{YBa}_2\text{Cu}_3\text{O}_7$). If the intersite Coulomb interaction $V_{pd}^z = V_{pd}^y$, is uniformly enhanced (see Fig. 6), the hole density at the apical oxygens increases. Enhancement of Δ_{pp} , anisotropic screening V_{pd}^z i.e., increase of the Cu(1)-O(4) Coulomb repulsion at constant intersite Coulomb interaction in chain direction V_{pd}^y or a decrease of t_{pp} , cause the opposite behavior (see Figs. 7 and 8). The dependence of the hole distribution on the other electron-electron interaction parameters U_d , U_p , and V_{pp} , within generally accepted bounds $7 \text{ eV} < U_d < 11 \text{ eV}$, $4 \text{ eV} < U_p < 6 \text{ eV}$, and $V_{pp} < 1 \text{ eV}$, is relatively weak (see, e.g., Fig. 9).

C. Spin-correlation function and comparison of the EDS with *ab initio* cluster calculations

For site energy differences $\Delta_{pd} \approx t_{pd}$ (i.e. tending towards the MV regime) our EDS-cluster calculations for the averaged charge densities,

$$\begin{aligned} \langle n_{\text{Cu}} \rangle &= \frac{1}{2}(n_{\text{Cu}(b)} + n_{\text{Cu}(d)}), \\ \langle n_{\text{O}_{\text{int}}} \rangle &= \frac{1}{3}(n_{\text{O}(a)} + 2n_{\text{O}(c)}), \end{aligned} \quad (11)$$

reveal more or less similar results compared with the *ab initio* LA cluster calculations of Mei and Stollhoff³⁷ (for site notation see Fig. 2). The density $\langle n_{\text{O}(4)+\text{O}(1)_{\text{end}}} \rangle$ shown in the last line of Table I is the average value over the chain terminating oxygens (e, e') and all apical oxygens.

In Fig. 10 we show the behavior of the spin-correlation function f_{ij} defined in Eq. (8) and that of the specific one \tilde{f}_{ij} , introduced by Mei and Stollhoff,³⁷ as

$$\tilde{f}_{ij} = \frac{\langle G | \vec{S}_i \vec{S}_j | G \rangle}{n_i n_j}, \quad i \neq j, \quad (12)$$

where the indices i, j count the sites on the chain axis (see Fig. 2). The diagonal part exceeds the off-diagonal components considerably. Since it is inconvenient to show both parts within one figure, the diagonal part has been omitted in Fig. 10.

For the central oxygen [site (a) in Fig. 2] the spin correlation function \tilde{f}_{aj} is negative for all j . The nearest-neighbor (NN) copper-copper spin correlations are negative and usu-

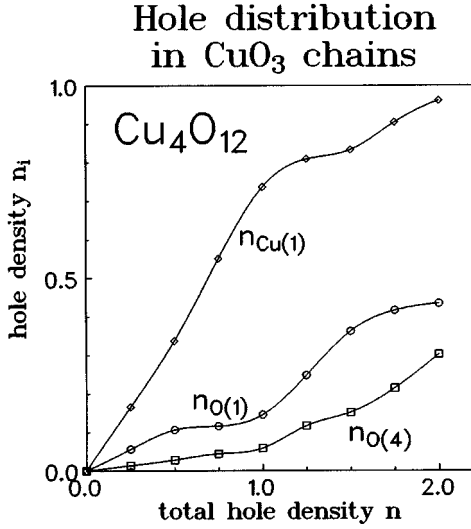


FIG. 4. Hole distribution vs total hole number for $0 \leq n \leq 2$. The adopted parameter set contains a modification of the set (II) with respect to different oxygen site energies $\Delta_{pp} = \varepsilon_p(O(4)) - \varepsilon_p(O(1)) = 1.4$ eV and $\Delta_{pd} = \varepsilon_p(O(1)) - \varepsilon_d = 3.6$ eV.

ally stronger than the NN copper-oxygen ones. There is one exception found in our EDS for the inner copper [site (b) in Fig. 1] for \tilde{f}_{bj} . The usual spin correlation function f_{ij} [Eq. (8)] does not show such behavior.

For the site (b) a sizable left-right asymmetry of \tilde{f}_{bj} can be seen at variance with a weak one, only, in Fig. 3(b) of Ref. 37. For next-nearest copper neighbors (NNN) they change to positive signs. Notable differences between our EDS and Ref. 37 occur for the oxygen-oxygen spin correlations \tilde{f}_{ij} . For the reference point (c) both of the NN and NNN oxygen-oxygen spin correlations are weak and negative in contrast to Ref. 37, where the NNN becomes ferromagnetic.

In general, copper-copper spin correlations (defined by \tilde{f}_{ij}) evaluated within the LA technique and our EDS show minor quantitative differences, whereas the NN oxygen-oxygen and NN copper-oxygen correlations according to our

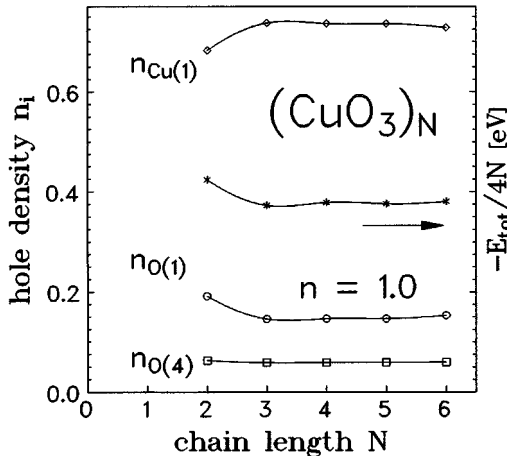


FIG. 5. Cluster size effect of the hole distributions for one hole per CuO_3 unit. The parameter set is the same as in Fig. 4.

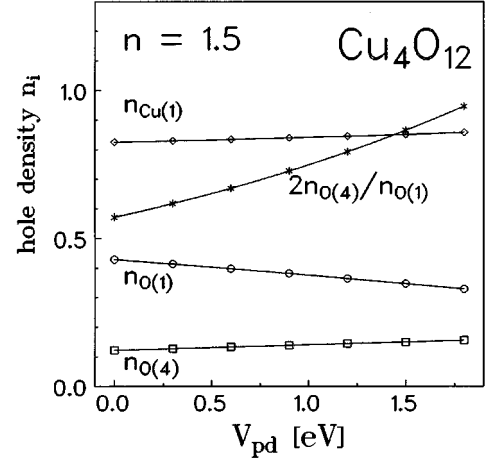


FIG. 6. Hole distribution in CuO_3 chains with $n = 1.5$ total holes per chain unit vs oxygen-copper Coulomb interaction V_{pd} . For the apical-chain oxygen site energy difference $\Delta_{pp} = \varepsilon_p(O(4)) - \varepsilon_p(O(1)) = 2$ eV has been adopted. The remaining parameters are taken from set (II) except slight modifications of the transfer integrals $t_{pd}^z = 1.42$ eV, $t_{pd}^y = 1.2$ eV and $t_{pp} = 0.6$ eV.

EDS results reveal sizably *weaker* values of about 50%. However, in our opinion, the stated lack of difference between oxygen and copper correlations³⁷ should be ascribed to a large extent to the specific form of the spin-correlation function given by Eq. (12). In fact, the small oxygen hole densities n_i (see Table I) introduced in its denominator compared with the spin-correlation function defined by Eq. (8) cause the stated equivalency. The behavior of the spin-correlation functions in the CT regime is similar, apart from some quantitative increase (weakening), for copper- (oxygen) centered functions (see Fig. 10).

In any case, the large charge gap $E_g \approx 2.1$ eV, the applicability of the antiferromagnetic spin-1/2 Heisenberg picture for the spin degrees of freedom, and the value of the corresponding exchange integral $J_{\text{ch}} \approx 140 - 190$ meV,^{29,30} i.e., comparable with that of layered cuprates, exclude at least for Sr_2CuO_3 a mixed-valency parameter regime.³⁴

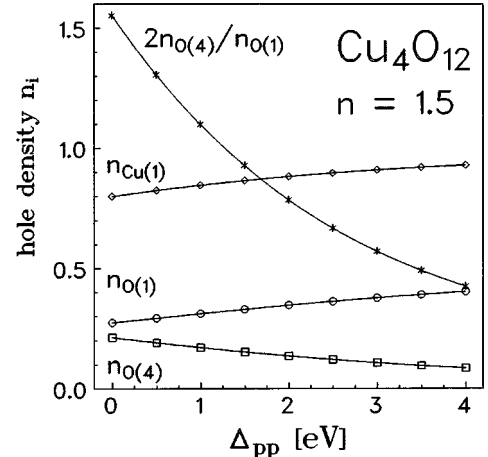


FIG. 7. The same as in Fig. 6 vs apical-chain oxygen site energy difference $\Delta_{pp} = \varepsilon_p(O(4)) - \varepsilon_p(O(1))$. For the remaining parameters see Fig. 6 and set (II).

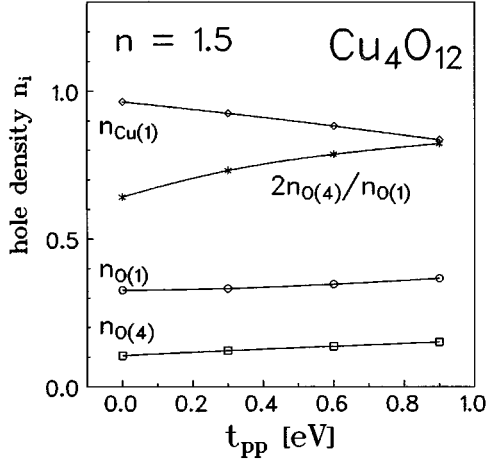


FIG. 8. The same as in Fig. 6 vs the apical-chain oxygen transfer integral t_{pp} .

D. $\text{YBa}_2\text{Cu}_3\text{O}_{x-\delta}$ family and comparison with O 1s XAS data

Interpreting the O 1s x-ray absorption spectroscopy (XAS) data, we consider the so-called prepeak contribution at energies below the transition into the upper Hubbard band at ≤ 530 eV for the electrical field \vec{E} directed \parallel to the axes a , b , c (see Figs. 6 and 9 of Ref. 1. Two edges for transitions polarized in \vec{a} and \vec{c} directions at 528.2 eV and at 527.2 eV, respectively, have been observed. They are ascribed to transitions into the $2p_x$ states of the plane oxygen O(2) and into the $2p_z$ states of the apical oxygen O(4), respectively. The difference spectrum “ $(\vec{E}\parallel b) - (\vec{E}\parallel a)$ ” shows an edge at 527.6 eV. Neglecting orthorhombic effects, i.e., the slight nonequivalence of planar O(2) and O(3) sites, the difference spectrum is ascribed to O(1) $2p_y$ states.¹ Within the same approximation the integrated cross section of the transition polarized $\vec{E}\parallel a$ direction ξ_a measures the oxygen partial density of holes doped into the planes $y_{O(2,3)}$. Let us start with the consideration of the orthorhombic-I phase. The total number of holes per CuO_2 unit considered in Sec. II, y , then reads

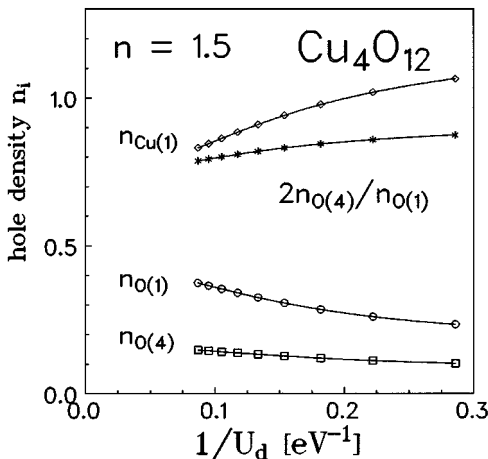


FIG. 9. The same as in Fig. 6 vs the copper on-site Coulomb interaction U_d .

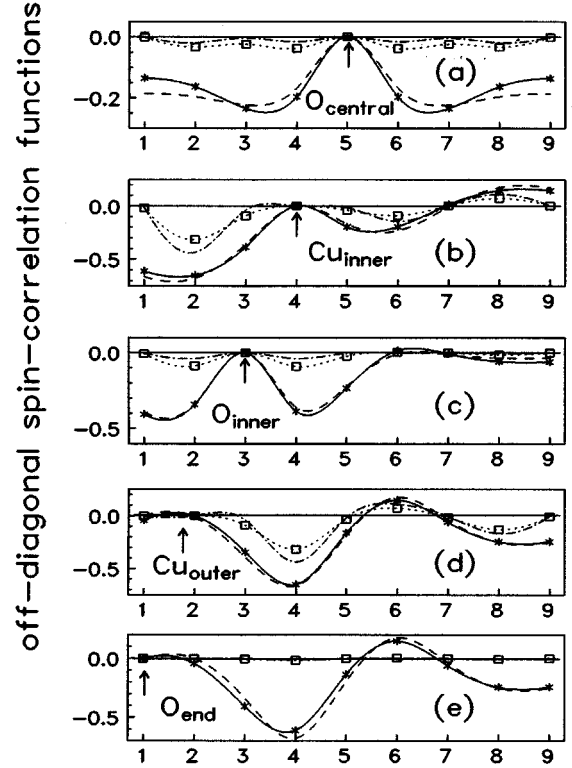


FIG. 10. Off-site spin-correlation functions [\square , according to Eq. (8); $*$, Eq. (12)] for an open Cu_4O_{13} cluster bearing four holes and $\Delta_{pd}=t_{pd}=1.2$ eV, $\Delta_{pp}=2$ eV. For the remaining parameters see text [set (II)]. The reference points are denoted by arrows: the central chain oxygen site (a), the inner copper site (b), the noncentral inner chain oxygen (c), the outer copper site (d), and the chain end oxygen sites (e, e'), (see Fig. 2). For comparison we also depict the ordinary spin-spin correlation function (\square and dotted line). The same functions for $\Delta_{pd}=3t_{pd}=3.6$ eV are denoted by dashed and dash-dotted lines, respectively.

$$y = \frac{(1 - \nu_1)\xi_a}{1 - \nu_2 + 2\xi_a(\nu_2 - \nu_1)} \approx \xi_a [1 + (\nu_2 - \nu_1)(1 - 2\xi_a)], \quad (13)$$

where the product $\nu_i y, i=1,2$, reveals the doped hole density at the i th Cu site (ν_2 is typically $\sim 0.15 - 0.2$). The “chain-plane site” difference is usually rather small: $|\nu_2 - \nu_1| \sim 0.05$. Thus, the uncertainty due to slightly differ-

TABLE I. Comparison of the averaged hole densities $\langle n_i \rangle$ obtained within the EDS and within the local ansatz approximation by Mei and Stollhoff (Ref. 37) for open Cu_4O_{13} clusters bearing four holes. In the EDS calculations different apical oxygen site energies Δ_{pp} (see text) and fixed chain oxygen copper site energy difference $\Delta_{pd}^h = t_{pd} = 1.2$ eV have been adopted. For the remaining parameters see set (II).

$\langle n_i \rangle$	Local ansatz	EDS		
		$\Delta_{pp}=2$ eV	$\Delta_{pp}=1$ eV	$\Delta_{pp}=0$
$\langle n_{\text{Cu}} \rangle$	0.43	0.395	0.441	0.499
$\langle n_{O(1)_{\text{int}}} \rangle$	0.38	0.287	0.276	0.258
$\langle n_{O(4)+O(1)_{\text{end}}} \rangle$	0.06	0.072	0.094	0.122

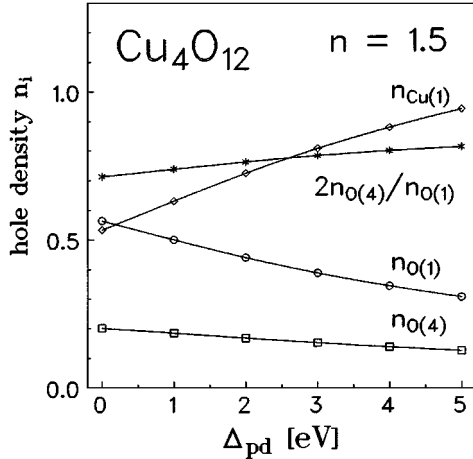


FIG. 11. The same as in Fig. 6 vs the site energy difference of chain oxygen and copper Δ_{pd} .

ent ν_1 values is much smaller than the experimental error bars for $\xi_a = 0.2 \pm 0.02$. With these numbers one arrives at $y = 0.2 \pm 0.026$.

Notice that the weak feature at $\delta = 0.85$ shown in Fig. 10 of Ref. 1 can be understood as the contribution from $(\text{Cu}_2\text{O}_5)^{-8}$ clusters. Small charges (holes) reside on the apical oxygens whereas each of the terminating copper ions bears large charges of $+1.99$.

The experimental ratio of holes at both apical oxygen sites relative to the chain oxygen sites amounts to about $2n_{\text{O}(4)}/n_{\text{O}(1)} = 0.76 \pm 0.12$ [XAS and electron energy loss spectroscopy (EELS), Ref. 1] and 0.93 derived from NMR data. For a reasonable intersite Coulomb interaction a sizable enhancement of the apical oxygen site energy by 1.5 to 2.5 eV is required to reproduce the experimental data (see Fig. 7). Due to the enhanced site energies at terminating apical oxygens [near O(1) vacancies], the lower half of this interval should be regarded as more realistic for ideal chains ($\delta = 0$). Finally, we note that our assumption of large Δ_{pd} values ~ 3 to 4 eV, clearly beyond the mixed-valency regime $\Delta_{pd} \leq t_{pd}$, found previously valid for Sr_2CuO_3 (Ref. 34) must be fulfilled for CuO_3 chains in $\text{YBa}_2\text{Cu}_3\text{O}_7$, too, in order to reproduce the XAS-derived hole densities (see Fig. 11).

To check the reliability of the extracted oxygen site energy differences, let us consider the experimental O 1s binding energy differences Δ_B^{el} . The differences of oxygen site energies (in electron representation) of $2p_\alpha$ states, $\alpha = x, y, z$, entering the plane and chain dp models are related to these quantities by

$$\begin{aligned} \Delta_{i\alpha,j\beta}^{\text{el}} &= \varepsilon_{2p_\alpha}^{\text{el}}(i) - \varepsilon_{2p_\beta}^{\text{el}}(j) = \Delta_{B,ij}^{\text{el}} + \Delta_{W_i,j}^{\text{el}} \\ &\approx \varepsilon_{1s}^{\text{el}}(i) - \varepsilon_{1s}^{\text{el}}(j) + \frac{e}{2} l^2 (V_i^{\alpha\alpha} - V_j^{\beta\beta}), \end{aligned} \quad (14)$$

where the indices $i, j = 1, 2, 3, 4$ have been taken in accordance with the notation of the oxygen sites. We recall that $i = 2, 3$ stands for the planar oxygens, $i = 1$ for the chain oxygen, and $i = 4$ for the apical oxygens. The first term on the right-hand side (RHS) of Eq. (14) describes approximately the crystal

field potential (difference) acting at the nucleus positions i and j . It can be taken directly from the XAS data. The second term accounts for the non-negligible spatial extent of the oxygen $2p$ Wannier functions. To first (crude) approximation it can be written as the energy difference of two point charges $0.5e$ residing at the centers of gravity of each of the two $2p_\alpha$ lobes, that is, at positions shifted by $l \sim 0.2 \text{ \AA}$ (for the estimate of l , see, e.g., Ref. 65) in directions α, β away from the corresponding nucleus position. The coefficients of this Taylor expansion are given by the corresponding components of the electrical field gradient tensor (EFG).

In the hole representation the apical-chain oxygen site energy difference $\Delta_{pp}^h \equiv \Delta_{41}$ reads

$$\Delta_{pp}^h = 4V_{pd}^y - 2V_{pd}^z + 4V_{pp} - \Delta_{pp}^{\text{el}}, \quad (15)$$

and the corresponding differences between the site energies of the apical oxygen O(4), the chain oxygen O(1), and the in-plane oxygen O(2) read, respectively,

$$\Delta_{42}^h \equiv \Delta_{a,pl}^h = 4V_{pd,pl}^y - 2V_{pd,ch}^z + 4V_{pp} - \Delta_{42}^{\text{el}}, \quad (16)$$

$$\Delta_{12}^h \equiv \Delta_{ch,pl}^h = 4(V_{pd,pl}^x - V_{pd,ch}^y) + 8(V_{pp}^l - V_{pp}^{\text{ch}}) - \Delta_{12}^{\text{el}}. \quad (17)$$

Adopting $V_{pp} = 0.5V_{pd}^y$ and $V_{pd}^z = V_{pd}^y = 1$ to 1.2 eV one obtains from Eqs. (14) and (15) $\Delta_{pp}^h = 3$ to $3.6 - 1.54 \text{ eV} \approx 2.5$ to 3 eV, where the XAS value of $\Delta_{41}^{\text{el}} = 0.4 \text{ eV}$ and the EFG values of $V_4^{zz} = 1.16 \times 10^{22} \text{ V/m}^2$, $V_1^{yy} = 1.73 \times 10^{22} \text{ V/m}^2$,⁶⁶ and $l = 0.2 \text{ \AA}$ have been used. This estimate of Δ_{pp}^h is in reasonable agreement with the value of 1.5 to 2.5 eV obtained above. For the difference Δ_{42}^h we estimate, from Eq. (16), 3 to $3.6 - 1 + 0.22 = 2.22$ to 2.82 eV, where $V_2^{xx} = 1.05 \times 10^{22} \text{ V/m}^2$ has been used. Then the energy $\varepsilon_{\text{apex}}$ becomes

$$\varepsilon_{\text{apex}} = \Delta_{pd,pl}^h + \Delta_{42}^h \sim 5 \text{ to } 6 \text{ eV}, \quad (18)$$

which is of fundamental interest for the parameter values of generalized t - J models or even for the stability problem of the Zhang-Rice singlet²¹ of the CuO_2 planes. Thus for $\text{YBa}_2\text{Cu}_3\text{O}_7$ the value of $\varepsilon_{\text{apex}}$ comes out very large. In other words, there is practically no destabilization effect caused by the apical oxygen in accord with the high critical temperature. In this case the standard three-band dp model and its reduction to the one-band t - J model reveal a sufficiently accurate low-energy description of the CuO_2 plane.

We note that the value of Δ_{pp} derived from the simulation of the charge transfer and the oxygen ordering by Aligia and Garcés³⁶ is about $2V_{pd}$ with the constraint $0.74t_{pd} < 2V_{pd} < 2.6t_{pd}$. In particular, in Ref. 7 a value of $\Delta_{pp} = 2.4 \text{ eV}$ has been adopted. This is in qualitative agreement with our results based on the simulation of the XAS data of Ref. 1. The relative positions of the O(1) $2p_y$ states and the planar $2p_{x,y}$ states which is of interest for the chain-plane charge transfer depends sensitively on the difference of $V_{pd,pl} - V_{pd,ch}$. A conceivable small difference of 0.1 eV, for example, caused by the puckering of the CuO_2 planes, reveals $\Delta\varepsilon_{12}^h \approx 0$ compared with 0.78 eV obtained for coinciding V_{pd} 's.

E. Some remarks on chain aspects of the $\text{PrBa}_2\text{Cu}_3\text{O}_7$ problem

The ionic radius analysis of various bond lengths in the 1-2-3 structure by Guillaume *et al.*⁶¹ suggests in linear extrapolation a mixed valency of Pr near +3.5, which is expected to be further reduced due to nonlinearities. The bond-valence analysis by Ramesh and Hegde⁶⁷ reveals +3.39. The stability of the ortho-II structure for $R=\text{Pr}$ compared with its absence for the neighboring rare earth $R=\text{Nd}$ ($r_{\text{Pr}(+3)} > r_{\text{Nd}(+3)} > r_{\text{Pr}(+4)}$) points also to a mixed valency state of Pr in between 3 and 4. From the persistence of the antiferromagnetic state of the Cu(2) subsystem and the magnitude of the corresponding Néel Temperature $T_N \sim 300$ K in $\text{PrBa}_2\text{Cu}_3\text{O}_6$ we estimated above the Pr valency to be less than 3.18.⁵⁹ Thus, the problem remains to elucidate where the missing holes (at least ≈ 0.16 per CuO_2 plane) reside now.

Let us discuss some related aspects for various $\text{PrBa}_2\text{Cu}_3\text{O}_7$ scenarios “explaining” its loss of superconductivity and metallicity by additional charge transfer to the chains on the basis of our results obtained above.

Within the hole doping chain scenario proposed by Khomskii²⁴ all σ -plane holes are pushed to the chain. In this case most of them should be located at the apical oxygen sites [see Figs. 3(b) and 4]. In principle, this should be detected by a sizable increase of the integrated cross sections ξ_c of the O 1s XAS absorption spectra with $\vec{E} \parallel c$ compared with the “difference spectrum” measured for $\vec{E} \parallel b$ and that for $\vec{E} \parallel a$ which is dominated by the transitions into the $2p_y$ states of the chain oxygen O(1). However, within an extended model which takes into account further electronic degrees of freedom as the planar Cu(2) $3d_{z^2}$ states having sizable overlap with the apical oxygen $2p_z$ states $t_{pd}^{zz} \sim 0.5$ eV,²¹ part of the additionally doped holes might be shifted back to the planes, but now into non- σ states. The O(4) $2p_z$ -Cu(2) $3d_{z^2}$ hybridization is effective only if the apical oxygen site energy $\varepsilon_{p_z} = \varepsilon_{\text{apex}}$ is reduced towards the corresponding Cu(2) site energy $\varepsilon_{3d_z^2}$ lying about 1 eV above the site energies of the Cu(2) $3d_{x^2-y^2}$ states. The corresponding difference amounts about 4 to 5 eV according to our analysis for $\text{YBa}_2\text{Cu}_3\text{O}_7$ presented in the previous section. In this context some hole depletion by the nontrivalent Pr and, more importantly, lowering of ε_{p_z} might be helpful or even necessary for the supposed additional plane-chain charge transfer itself. According to Fig. 7 a corresponding decrease of Δ_{pp} is accompanied by a reduction of the hole density $n_{\text{O}(1)}$ at the O(1) $2p_y$ states. In other words, then, the characteristic strong yz asymmetry of the hole distribution surrounding the Cu(1) site of regular R -1-2-3 superconductors is reduced. This might be of interest for the interpretation of recent nuclear quadrupole resonance (NQR) data of $\text{PrBa}_2\text{Cu}_3\text{O}_7$ and $\text{GdBa}_2\text{Cu}_3\text{O}_7$ by Nehrke *et al.*⁶⁸ where some reduction of the Cu(1) EFG anisotropy parameter $\eta = (|V^{zz} - V^{yy}|)/|V^{xx}|$ from 0.8 ± 0.15 to 1 ($\text{GdBa}_2\text{Cu}_3\text{O}_7$) and a nearly constant main EFG tensor component for both compounds have been reported. (Here we have assumed that the latter is given in both cases by the V^{xx} component as suggested by local symmetry.)

For completeness, we note that according to Figs. 3(a) and 4 up to ≈ 0.1 holes can be shifted to the Cu(1) $3d_{z^2-y^2}$ states ongoing from $n=1.5$ to $n=2$. Thus, within this scenario, a non-negligible part of holes shifted to Cu(2) and Cu(1) states could not be detected by the O 1s XAS measurements on principle. However, the latter possibility is unlikely with respect to the mentioned Cu(1) NQR data.⁶⁸

According to the reflectivity data of Takenaka *et al.*⁶⁹ approximately the same effective charge (about 0.5 electrons) reside in the CuO_3 chains of $\text{YBa}_2\text{Cu}_3\text{O}_7$ and of $\text{PrBa}_2\text{Cu}_3\text{O}_7$ as well. Just this result (together with other experimental data suggesting a Pr valency close to +3) was the starting point for the construction of the Pr $4f$ -O $2p$ π -hybridization model by Fehrenbacher and Rice.⁵⁰ In subsequent papers by Fehrenbacher⁶ and Aligia *et al.*⁷ the t - J model has been adopted to describe quantitatively the optical conductivity of CuO_3 chains of both compounds in the low-frequency region $\omega \leq 1$ to 1.4 eV. From the f -sum rule of the t - J model they get $n_{\text{eff}} = 2 - n = 0.43$ to 0.45 and $t_{\text{eff}} = 0.4$ eV for $\text{YBa}_2\text{Cu}_3\text{O}_7$ (Ref. 6) compared with $n_{\text{Pr}}^{\text{Pr}} = 0.451$, $n_{\text{eff}}^{\text{Y}} = 0.5$ and $t_{\text{eff}} = 0.85$ eV obtained in Ref. 7 from the mapping of $\sigma(\omega)$ of the four-band dp model [open $(\text{CuO}_2)_4\text{O}_3$ cluster] on the conductivity of a chain with four sites and open boundary conditions bearing noninteracting spinless fermions.⁷⁰ However, according to our results presented in Sec. IV A the DOE approximation for the $3d$ Cu orbital (or any other effective orbital in corresponding reduced models) works well for light doping only (see Fig. 3). Since the DOE approximation is the basis of the t - J models, uncertainties up to 25% might occur for the case $n=2$.⁷¹ In this context we note that serious difficulties in extracting quantitative information from the application of sum rules of reduced Hamiltonians have been stressed in Ref. 72.

F. Possible long-range-ordered states of CuO_3 chain compounds

The elucidation of the nature of the ground state of the CuO_3 chains in differently doped states is a very intriguing but subtle issue, with respect to the interpretation of recent experimental data listed in Sec. I and below as well as with respect to some general problems in cuprate physics as well. In this connection we remind the reader that the dp model has no electron-hole symmetry. This is important for the explanation of the well-known asymmetry of the phase diagram of layered cuprates with respect to hole and electron doping. Is there an analogous effect in one dimension (1D)? What is the nature of the superconducting state observed in CuO_3 chains at a doping level exceeding almost twice the upper critical doping ratio in CuO_2 planes, etc.?

Strictly speaking, in one dimension there are no ordered states. However, several phases such as charge-density-wave (CDW) states have large correlation lengths and for many practical purposes they behave as having long-range ordered states on finite systems. In some cases 3D ordering for macroscopic systems at finite temperature is established due to the weak interchain coupling always present in real solids.

The usual way to look, e.g., for superstructures consists in the computation of Fourier transforms of the corresponding correlation functions $S_{\mu}(q)$, where μ specifies the ordered state (e.g., spin-spin, etc.). Then, from a clear maximum or a

cusps at finite chain lengths, regarded as a precursor of a divergency in the infinite (coupled) chain limit, the period and the nature of the ground state can be deduced (see, e.g., Ref. 78). Another approach is based on the analysis of the slowest decay of various correlations against distance. At first glance, it might seem that the 1D character of the model under consideration and the relatively large number of sites $N \sim 16$ to 24 involved in our EDS provide a safe basis to perform corresponding studies. However, the relevant number of chain units $\mathcal{N}_c = N/4$ is still too small to extract reliable information about the long-range-ordered states expected. At most some hints for possible long-range-ordered phases can be obtained.

As an example we shall consider the magnetic or spin structure factor $S_\sigma^{zz}(q)$, as usual defined by

$$S_\sigma^{zz}(q) = \frac{1}{\mathcal{N}_c} \sum_{i,j} e^{i\vec{q}(\vec{r}_i - \vec{r}_j)} \langle G | S_i^z S_j^z | G \rangle, \quad (19)$$

for the cases $n=0.5$, $n=1$, and $n=1.5$. The latter two hole concentrations are of interest for Sr_2CuO_3 and $\text{YBa}_2\text{Cu}_3\text{O}_7$, respectively, as discussed above. In Eq. (19), S_i^z, S_j^z denote the z components of the total spin of the unit cells i, j , respectively. In small systems as are considered here, only a limited set of wave vectors \vec{q} has significance. Using Eq. (8), we evaluated $S_\sigma^{zz}(0)$, $S_\sigma^{zz}(\pi/2b)$, and $S_\sigma^{zz}(\pi/b)$ for $\mathcal{N}_c=4$ and the parameter set explained in Fig. 4. In the case $n=1$ we obtained a dominant $2k_F \equiv \pi/b$ -contribution as expected:

$$S_\sigma^{zz}(0) = 0.0 \ll S_\sigma^{zz}(\pi/2b) = 0.1635 \ll S_\sigma^{zz}(\pi/b) = 0.5364,$$

which is regarded as the precursor of a $2k_F$ spin-density-wave (SDW) phase detected in recent neutron scattering studies of Sr_2CuO_3 below 5.4 K.⁷⁹ Naturally, due to the smaller cluster size, the value of $S_\sigma^{zz}(\pi/b)$ is smaller than $S_H^{zz}(\pi/b) \approx 1.23$ found by Ogata and Shiba in the related Heisenberg case (26 sites) (Ref. 80) and the diverging infinite chain approximations

$$\lim_{\mathcal{N}_c \rightarrow \infty} S_H^{zz}(q) \rightarrow \approx 0.232 \ln \{ [1 + \sin(q/2b)] / \cos(q/2b) \}, \quad (20)$$

or similarly [see Ref. 81 (28 sites) and references therein]

$$S_H^{zz}(q) = -0.25 \ln(1 - q/\pi b). \quad (21)$$

Naturally, our value of $S_\sigma^{zz}(\pi/b)$ does not exceed the corresponding Heisenberg model value for four spins: $S_H^{zz}(\pi/b) = 2/3$. Our four-band value of $S_\sigma^{zz}(\pi/b)$ nearly coincides with the corresponding values ≈ 0.8 quoted by Meinders for an eight-site periodic ring of the one-band extended Hubbard model ($U/t=10$, $V/t \leq 1$) (Ref. 82) and with $\approx 0.72 - 0.74$ for a hexagon and an octagon, respectively, treated within the simple one-band Hubbard model at $U/t=10$ (see Callaway *et al.*⁸³). The $S_\sigma^{zz}(\pi/2b)$ value is larger (smaller) than the corresponding long-chain Heisenberg quantities ≈ 0.165 , 0.2045 , and 0.1733 given in Ref. 80 and following from Eqs. (20) and (21), respectively.

For electron doping $n=0.5$ we obtained, again as expected, a dominant $2k_F$ contribution $S_\sigma^{zz}(q = \pi/2b) = 0.1756$

and a smaller $4k_F$ one: 0.1276 , which should be compared with similar numbers 0.2471 and 0.125 obtained in Ref. 80 for the quarter-filled periodic Hubbard rings with 32 sites in the strongly correlated limit $U/t \rightarrow \infty$. However, in the case of hole doping, i.e., for $n=1.5$, the $2k_F (q = \pi/2b)$ contribution $S_\sigma^{zz}(\pi/2b) = 0.2062$ remains yet slightly smaller than the $4k_F$ one: 0.2431 . The reason for this unexpected behavior is unclear at present. The results for $n=0.5$ and $n=1$ are in qualitative accord with the results of the 1D- t - J -model in the limit $t/J \ll 2$. In fact, the simulation of the exchange integral J and the charge gap for Sr_2CuO_3 within the simple one-band Hubbard model yields $U/t \approx 9$ and $t \approx 0.34$ eV. Hence, $J/t \sim 0.5$ can be estimated. In sharp contrast, for $n=1.5$ an unexpectedly large ratio $2 < J/t \leq 2.5$ should be adopted comparing our results with the Monte Carlo calculations of the 1D t - J model by Assad and Würtz⁸⁴ (performed for 32 and 24 sites) to get $1.2 S_\sigma^{zz}(\pi/2b) \approx S_\sigma^{zz}(\pi/b)$. Possibly, a generalized asymmetric $t-t''$ - J - V model like in Ref. 85 provides a better description of hole doped CuO_3 chains.

Although our result might be strongly affected by the small ring size leading to a smearing of the leading ‘‘ $2k_F$ singularity,’’ it nevertheless reflects a remarkable magnetic e - h asymmetry resembling the well-known asymmetric phase diagram for doped layered cuprates. To summarize, for electron-doped quarter-filled 1D cuprates a $2k_F$ SDW can be expected, whereas the magnetic structure of long quarter-filled hole-doped CuO_3 chains remains unclear.

Similar problems arise at $n=1.5$ for the charge structure factor $S_\rho(q)$ defined analogously to Eq. (19) replacing the spin operators S_i^z by the charge density operators n_i . No definite conclusions with respect to a solely electronically driven CDW or (superconducting) state can be drawn for a weak short-ranged intersite Coulomb interaction $V_{pd} \sim 1$ eV. All these problems can be settled in principle, at least partially, using other many-body techniques such as quantum Monte Carlo or the density renormalization group method (see, e.g., Refs. 86 and 81).

Another possibility to circumvent these difficulties is to map the present four-band extended Hubbard model onto a reduced Hamiltonian for which larger chains can be diagonalized and/or its long-range behavior is already known. Within such an approach we have shown that the present Hamiltonian with nearly standard CuO_2 -plane-derived parameters can be mapped approximately onto an antiferromagnetic spin-1/2 Heisenberg model³⁴ (predicting correctly the value of the exchange integral J_{ch} for Sr_2CuO_3), a one- and onto a two-band extended Hubbard model for $n=1$ and analogously also for $n=1.5$.⁸⁷

Acting along these lines, we do not try to solve the ground state problem of CuO_3 chains; instead, analyzing available experimental data, we want only to restrict the possible parameter space, leaving its final solution for future work. Concerning $\text{YBa}_2\text{Cu}_3\text{O}_7$, we recall that due to the direct contact between chains and planes this problem is further complicated since any phase transition in one subsystem changing the common chemical potential might cause additional charge transfer to the other one. Hence, strictly speaking, even the band filling of one isolated chain is not well defined.

Returning to the CDW problem, we note that, more importantly, the electron-lattice interaction ignored in the present paper can seriously affect the charge or bond ordering of the ground state. Adopting the adiabatic approximation, we obtained by self-consistent calculations in some cases strong amplification of $4k_F$ CDW correlations leading to ordered states, at least in finite clusters. In other cases the former were suppressed in favor of $2k_F$ -ordered states. In particular, for $n=1$ we obtained within our single-chain approach some hints for a weak spin-Peierls state with a dimerization amplitude $u_0 \sim 10^{-2} - 10^{-3} \text{ \AA}$ (see also the discussion of experimental data given below). Within the present four-band dp model, such a state is characterized by a Cu-Cu bond order wave (BOW) accompanied by a very weak CDW on the chain oxygen O(1) sites, i.e., a $2k_F$ mixed CDW-BOW state. For $n=1.5$ and parameters in the strongly correlated regime as adopted here, we have found a $4k_F$ mixed CDW-BOW state, quite similar to the $2k_F$ CDW-BOW state obtained within the one-particle approach at half-filling.^{17,34} This CDW-BOW state is characterized by the alternation of two shortened and two enlarged Cu-O bonds in the chain direction. The CDW yields differently charged Cu-O₂ radicals [involving the two apical oxygens O(4)] and equally charged chain oxygens O(1). Depending on the sign of the diagonal electron-lattice interaction, the transverse O(4)-Cu(1)-O(4) bonds are shortened and enlarged (vice versa), too. In contrast, a mixed $2k_F$ CDW-BOW state, where all bonds and local charges are affected by the superstructure formation, can be obtained for a weakly to medium correlated parameter regime and strong electron-lattice interactions derived from a linear combination of atomic orbitals (LCAO) deformation study of YBa₂Cu₃O₇.¹⁸ In principle, such a situation cannot be excluded for a highly doped chain in the vicinity of the metallic planes of YBa₂Cu₃O₇ where their screening might reduce the strong on-site interactions generic for undoped Sr₂CuO₃.

Experimentally, the situation for YBa₂Cu₃O₇ is yet quite controversial and unclear. While recent surface-sensitive scanning tunneling microscopy (STM) data by Edwards *et al.*³ have been interpreted in terms of a CDW or SDW with a period of $(3.3 \pm 0.3)b$, no CDW could be detected within a special x-ray scattering search.⁸⁸ Evidence for one-dimensional chain related fluctuations, i.e., to a dynamical CDW or BOW with a period of $\approx 4.28b$, i.e., near a $2k_F$ structure, has been deduced from inelastic neutron scattering data by Mook *et al.*⁵ Similarly, a near $2k_F$ CDW or SDW has been deduced also from Doppler-broadened positron annihilation radiation (DBAR) spectral data by Huang *et al.*⁴ The possible absence of a spin-Peierls phase for undoped Sr₂CuO₃ Ref. 27 might be related to significant interchain exchange (in a direction stabilizing the Néel state below $T_N \approx 4 - 6 \text{ K}$ (compare Refs. 89 and 90 for general theoretical aspects).

At this stage we shall stop the discussion of possible long-range-ordered states of CuO₃ chains since it is not the central scope of the present paper. For more detailed information, the interested reader is referred to our published papers mentioned above and to forthcoming work in preparation.⁸⁷ We stress that the main conclusions based on the O 1s XAS-derived oxygen hole distribution and the related parameter set are only slightly affected by the presence or absence of

any CDW-BOW state since (i) these measurements yield a site specific hole content averaged over the whole crystal, i.e., averaged also over the superstructure period, and (ii) the redistribution of charge between copper and oxygen sites after the onset of the CDW-BOW state has been found to be small for all considered self-consistent solutions. Roughly it is one order of magnitude smaller than the CDW amplitude itself, i.e., yet within the experimental error bars.

Finally, we believe that the error induced by the assumption that the calculated oxygen hole densities are essentially related to mobile holes only is of the same order of magnitude. This is based on the experimental observation that no upper Hubbard band contribution has been observed for strongly doped chains. In addition recent calculation of Eskes and Oles⁹¹ and Ref. 72 give further support for such a point of view. For example, in Ref. 91 it was shown for the case of the one-dimensional simple Hubbard model that the upper Hubbard band loses its weight rapidly with increasing doping content. Thus, for a doping ratio of ~ 0.5 its contribution to the integrated conductivity and some one-particle spectra is smaller than 5% of the total weight.

V. SUMMARY

The four-band dp model with minor changes in CuO₂-plane-derived parameter sets yields a reasonable description of available experimental data for a variety of compounds containing CuO₃ chains with different filling ratios. This enabled us to analyze critically various approaches to materials of current interest such as (Sr,Ca)₂CuO₃, YBa₂CuO₃O_{7- δ} , $\delta \approx 0,0.5$, and PrBa₂Cu₃O₇. In addition, at least for the YBCO systems within intact chains, sizably enhanced apical oxygen site energies compared with the chain oxygen ones are necessary to describe details of the hole distributions between them. Detailed predictions of the hole distributions among copper and oxygen sites within these chains are made provided a substantial hole- or electron-doped chain mechanism is involved in the destruction of superconductivity and metallicity in PrBa₂Cu₃O₇.

The large concentration of doped mobile holes realized in typical CuO₃-chains of the RBa₂Cu₃O_{7- δ} family compared with layered cuprates causes a unique situation where well-known theoretical approaches starting either from the quasi-particle picture within a self-consistent field description or from highly correlated states excluding double occupancy lead to sizable and comparable deviations of the order 10 - 20 % compared with our EDS local charge densities: negative for the Cu(1) site and positive for both oxygens O(1) and O(4). Within the charge transfer limit $U_d \gg \Delta_{pd} \gg t_{pd}$ for $1 \leq n \leq 1.5$ holes per chain period, relevant for (Ca,Sr)₂CuO₃ and its doped derivatives, a sizable difference of our exact diagonalization results compared with the predictions of the local ansatz and the Hartree-Fock approximation has been found. For sizable hole doping or a mixed valency parameter regime and even for half-filling $n=1$ only minor deviations occur. For realistic, slightly modified CuO₂-plane-derived parameter sets, approaches which make use of the exclusion of double occupancy becomes less accurate with increasing doping content.

The magnetic structure factor $S_{\sigma}^{zz}(q)$ exhibits for one-quarter-filled (mobile) electron- and hole-doped chains a re-

markable asymmetry with respect to the weights at $2k_F$ and $4k_F$. The experimental investigation of electron-doped CuO_3 chains, not reported so far to our knowledge, would be of considerable interest.

Note added in proof. In a recent paper by H. Suzuura *et al.* [Phys. Rev. Lett. **76**, 2579 (1996)] on the mid-infrared optical absorption of Sr_2CuO_3 (Ca_2CuO_3), an asymmetric cusp-like structure near 0.48 (0.47) eV has been reported. Analyzing these data in terms of the phonon-assisted magnetic absorption model, they estimated an unexpectedly large exchange integral $J_{\text{ch}} \approx 0.26$ eV, at variance with the analysis of the magnetic susceptibility data given in Refs. 29, 30, and 34 pointing to $J_{\text{ch}} \approx 0.2$ eV. Our calculations in Ref. 34 have been performed adopting $\Delta\epsilon_{pd} = 3.5$ to 3.6 eV and the constraint of a large charge transfer gap of $E_g = 2.1$ eV reported for Ca_2CuO_3 in Ref. 26. However, some recent theoretical and experimental hints [Okada *et al.*, J. Phys. Soc. Jpn. **65**, 1844 (1996)] indicate that at least for Sr_2CuO_3 the values of $\Delta\epsilon_{pd}$ and E_g might be significantly smaller. The search for an improved dp -parameter set and for a suitable reduced

model Hamiltonian to describe the above mentioned experimental data will be addressed in a forthcoming paper.

ACKNOWLEDGMENTS

Discussions with Professor J. Fink, Professor P. Fulde, Professor W. Hanke, Professor D. Khomskii, Professor A.F. Barabanov, Professor G. Stollhoff, Professor H. J. Schulz, Professor H. Fukuyama, Dr. K. Rościszewski, Dr. M. Knupper, Dr. P. Knoll, Dr. R. Hayn, Dr. R. Schumann, Dr. K. Dichtel, and Dr. M. Merz are gratefully acknowledged. Special thanks goes to Dr. M.S. Golden for discussions and a critical reading of the manuscript. One of us (J.M.) thanks the Max-Planck-Arbeitsgruppe "Elektronensysteme" at the Technical University Dresden for hospitality during which part of the present work was performed. Finally, the Deutsche Forschungsgemeinschaft is also acknowledged for financial support (S.-L.D. and J.M.) under Project No. Dre-269/5-1.

*Author to whom all correspondence should be addressed. Electronic address: drechsler@ifw-dresden.d400.de

[†]On leave from Institute of Physics, Prague, Czech Republic.

- ¹N. Nücker, E. Pellegrin, P. Schweiss, J. Fink, S.L. Molodtsov, C.T. Simons, G. Kaindl, W. Frentrop, C. Thomsen, A. Erb, and G. Müller-Vogt, Phys. Rev. B **51**, 8529 (1995).
- ²H.L. Edwards, D.J. Derro, A.L. Barr, J.T. Markert, and A.L. de Lozanne, Phys. Rev. Lett. **75**, 1387 (1994).
- ³H.L. Edwards, A.L. Barr, J.T. Markert, and A.L. de Lozanne, Phys. Rev. Lett. **73**, 1154 (1994).
- ⁴W.F. Huang, Z.R. Xu, S.H. Liu, and M.P. Wu, Phys. Rev. B **41**, 2052 (1990).
- ⁵H. Mook, P. Dai, K. Salama, D. Lee, F. Dogan, G. Aeppli, A. Boothroyd, and M.E. Mostoller, Phys. Rev. Lett. **77**, 370 (1996).
- ⁶R. Fehrenbacher, Phys. Rev. B **49**, 12 230 (1994).
- ⁷A.A. Aligia, E.R. Gagliano, and P. Vairus, Phys. Rev. B **52**, 13 601 (1995).
- ⁸P. Gawiec, D. Grepel, A. Riiser, H. Haugerud, and G. Uimin, Phys. Rev. B **53**, 5872 (1996).
- ⁹P. Gawiec, D. Grepel, G. Uimin, and J. Zittartz, Phys. Rev. B **53**, 5880 (1996).
- ¹⁰W.A. Atkinson and J.P. Carbotte, Phys. Rev. B **52**, 10 601 (1995).
- ¹¹R. Bernhard, Ch. Niedermayer, U. Binninger, A. Hofer, Ch. Wenger, J.L. Tallon, G.V.M. Williams, E.J. Ansaldo, J.I. Budnick, C.E. Stronach, D.R. Noakes, and M.A. Blankson-Mills, Phys. Rev. B **52**, 10 488 (1995).
- ¹²V. Breit, P. Schweiss, R. Hauff, H. Wühl, H. Claus, H. Rietschel, A. Erb, and G. Müller-Vogt, Phys. Rev. B **52**, R15 727 (1995).
- ¹³D.N. Basov, R. Liang, D.A. Bonn, W.N. Hardy, B. Dabrowski, M. Quijada, D.B. Tanner, J.P. Rice, D.M. Ginsberg, and T. Timusk, Phys. Rev. Lett. **74**, 598 (1995); J. Münzel, A. Zibold, H.P. Geserich, and Th. Wolf, Europhys. Lett. **33**, 147 (1996).
- ¹⁴In this case a small gap would be induced in the chain subsystem and the temperature dependence of the penetration depths should be different for the a and b directions. The former is determined by the large gap only. However, the observed anisotropy of the planar penetration depths in a and b (chain) directions does not depend on temperature.

- ¹⁵H. Eschrig and S.-L. Drechsler, Physica C **173**, 80 (1991).
- ¹⁶S.-L. Drechsler, J. Malek, and H. Eschrig, Synth. Met. **57**, 4626 (1993).
- ¹⁷S.-L. Drechsler, J. Malek, M.Yu. Lavrentiev, and H. Köppel, Phys. Rev. B, **49**, 233 (1994).
- ¹⁸J. Paulsen, H. Eschrig, S.-L. Drechsler, and J. Malek, in *Anharmonic Properties of High- T_c Cuprates*, edited by D.D. Mihailovic, G. Ruani, E. Kaldis, and K.A. Müller (World Scientific, Singapore, 1995), pp. 95–104.
- ¹⁹M.I. Salkola, A.R. Bishop, J. Mustre de Leon, and S.A. Trugman, Phys. Rev. B **49** 3671 (1994).
- ²⁰Y. Ohta, T. Tohyama, and S. Maekawa, Phys. Rev. B **43**, 2968 (1991).
- ²¹R. Raimondi, J.H. Jefferson, and L. Feiner (unpublished); C. Di Castro, L.F. Feiner, and M. Grilli, Phys. Rev. Lett. **66**, 3209 (1991); L.F. Feiner, M. Grilli, and C. Di Castro, Phys. Rev. B **45**, 10 647 (1992).
- ²²M.P. López Sancho, J. Rubio, M.C. Refolio, and J.M. López Sancho, J. Phys. Condens. Matter **6**, L29 (1994).
- ²³Kh. Eid, M. Matlak, and J. Zielinski, Physica C **220**, 61 (1994).
- ²⁴D. Khomskii, J. Supercond. **6**, 69 (1993).
- ²⁵In-Sang Yang, A.G. Schrott, and C.C. Tsuei, Phys. Rev. B, **41**, 8921 (1990); Physica C **6**, 69 (1994).
- ²⁶M. Yoshida, S. Tajima, N. Koshizuka, S. Tanaka, S. Uchida, and S. Ishibashi, Phys. Rev. B **44**, 11 997 (1991); Y. Tokura, S. Koshihara, T. Arima, H. Takagi, S. Ishibashi, T. Ido, and S. Uchida, *ibid.* **41**, 11 657 (1990); O. Misochko, S. Tajima, C. Urano, H. Eisaki, and S. Uchida, *ibid.* **53**, R14 733 (1996).
- ²⁷A. Keren, L.P. Le, G.M. Luke, B.J. Sternlieb, W.D. Wu, Y.J. Uemura, S. Tajima, and S. Uchida, Phys. Rev. B **48**, 12 926 (1993).
- ²⁸T. Ami, M.K. Crawford, R.L. Harlow, Z.R. Wang, D.C. Johnston, Q. Huang, and R. Erwin, Phys. Rev. B **51**, 5994 (1995).
- ²⁹S. Eggert, Phys. Rev. B **53**, 5116 (1996).
- ³⁰N. Motoyama, H. Eisaki, and S. Uchida, Phys. Rev. Lett. **76**, 3212 (1996); M. Takigawa, N. Motoyama, H. Eisaki, and S. Uchida, *ibid.* **76**, 4612 (1996).
- ³¹A. Simon, H. Borrmann, W. Bauhofer, R.K. Kremer, and H. Mat-

- tausch, in *High- T_c Superconductors*, edited by H.W. Weber (Plenum New York, (1988).
- ³²Y.J. Shin, E.D. Manova, J.M. Dance, P. Dordor, J.C. Grenier, E. Marquestaut, J.P. Doumerc, M. Pouchard, and P. Hagenmuller, *Z. Anorg. Allg. Chem.* **616**, 201 (1992).
- ³³W.B. Archibald, J.S. Zhou, and J. Goodenough, *Phys. Rev. B* **52**, 16 101 (1995).
- ³⁴S.-L. Drechsler, J. Malek, S. Zalis, and K. Rościszewski, *Phys. Rev. B* **53**, 11 328 (1996); *J. Supercond.* **9**, 439 (1996).
- ³⁵A.M. Oleś and W. Grzelka, *Phys. Rev. B* **44**, 9531 (1991).
- ³⁶A.A. Aligia and J. Garcés, *Phys. Rev. B* **49**, 524 (1994).
- ³⁷C.-J. Mei and G. Stollhoff, *Phys. Rev. B* **43**, 3065 (1991).
- ³⁸M. Hybertsen, E. Stechel, M. Schluter, and D. Jennison, *Phys. Rev. B* **41**, 11 068 (1990).
- ³⁹A.K. McMahan, J.F. Annett, and R.M. Martin, *Phys. Rev. B* **42**, 6268 (1990).
- ⁴⁰F. Mila, *Phys. Rev. B* **38**, 11 358 (1988).
- ⁴¹G. H. Eskes, G. Sawatzky, and L. Feiner, *Physica C* **41**, 424 (1989).
- ⁴²M. Maple, C. Almasan, C. Seaman, S. Han, K. Yoshiara, M. Buchgeister, L. Paulius, B. Lee, D. Gajewski, R.F. Jardim, C.R. Fincher, G. Blanchet, and R.P. Guertin, *J. Supercond.* **7**, 97 (1994).
- ⁴³P. de Groot, T. Young, B. Rainford, M. Weller, J. Grasmeyer, and O. Schärpf, *Physica C* **185-189**, 1169 (1991).
- ⁴⁴In the recent work of V. Ponnambalam and U.V. Varadaraju, *Phys. Rev. B* **52**, 16 213 (1995), for stoichiometric $\text{YBaLaCu}_3\text{O}_{7+\delta}$ an excess oxygen content of $\delta=0.07$ and tetragonal symmetry have been reported. We assume that locally the chain structure of the basal plane is retained.
- ⁴⁵J. Zaanen, A.T. Paxton, O. Jepsen, and O.K. Andersen, *Phys. Rev. Lett.* **60**, 2685 (1988).
- ⁴⁶H. Schiefer, M. Mali, J. Roos, H. Zimmermann, and D. Brinkmann, *Physica C* **162-164**, 171 (1989).
- ⁴⁷M. Muroi and R. Street, *Physica C* **246**, 357 (1995).
- ⁴⁸H. Lütgemeier and I. Heinmaa, in *Phase Separation*, edited by K.A. Müller and K. Benedek (World Scientific, Singapore, 1993), p. 242; H. Lütgemeier, I. Heinmaa, D. Wagener, and S.M. Hosseini, in *Phase Separation in Cuprate Superconductors*, edited by E. Sigmund and K.A. Müller (Springer-Verlag, Berlin, 1994), p. 224.
- ⁴⁹Thus, for example, the Hall data of Z.Z. Wang, J. Clayhold, N.P. Ong, J.M. Tarascon, L.H. Greene, W.R. McKinnon, and G.W. Hull, *Phys. Rev. B* **36**, 7222 (1987), at 100 K yield $y=0.24$ at $\delta=0$ and $y=0.155$ at $\delta=0.1$ compared with 0.22 and $y=0.175$ obtained from Eqs. (1) and (2), respectively.
- ⁵⁰R. Fehrenbacher and M. Rice, *Phys. Rev. Lett.* **70**, 3471 (1993).
- ⁵¹M. Biagini, C. Calandra, and S. Ossicini, *Phys. Rev. B* **52**, 10 468 (1995).
- ⁵²D. Singh, *Phys. Rev. B* **50**, 4106 (1994).
- ⁵³E. Kuzmann, M. Gal, Z. Homonnay, S. Nagy, Gy. Vanko, and A. Vertes, *Hyperfine Interact.* **93**, 1621 (1994).
- ⁵⁴K. Widder, M. Merz, D. Berner, J. Münzel, H. P. Gesserich, A. Erb, R. Flükiger, W. Widder, and H. F. Braun, *Physica C* **264**, 11 (1996).
- ⁵⁵J. Tallon, C. Bernhard, U. Binniger, A. Hofer, G. Williams, E.J. Ansaldo, J.I. Budnick, and Ch. Niedermayer, *Phys. Rev. Lett.* **74**, 1008 (1995); J. Tallon, C. Bernhard, H. Shaked, R.L. Hitterman, and J.D. Jorgensen, *Phys. Rev. B* **51**, 12 911 (1995).
- ⁵⁶G. Zheng, Y. Kitaoka, K. Ishida, and K. Asayama, *J. Phys. Soc. Jpn.* **64**, 2524 (1995).
- ⁵⁷R.P. Gupta and M. Gupta, *Phys. Rev. B* **45**, 9958 (1992).
- ⁵⁸P. Schlegler, H. Casalta, R. Hadfield, H.F. Poulsen, M. v. Zimmermann, N.H. Andersen, J.R. Schneider, R. Liang, P. Dosanjh, and W.N. Hardy, *Physica C* **241**, 103 (1995).
- ⁵⁹Adopting Ba^{+2} and the same valency of Pr in $\text{PrBa}_2\text{Cu}_3\text{O}_6$ as well as in $\text{PrBa}_2\text{Cu}_3\text{O}_7$, we argue that any valency exceeding +3 leads to *electron* doping of the CuO_2 planes at least in the former case. From the minimal electron concentration for the occurrence of superconductivity $-y=n_{el}\approx 0.13$ in the electron-doped compound $\text{Nd}_{2-x}\text{Ce}_x\text{CuO}_4$ one then estimates $z<0.26$. A smaller value of this upper bound $z\approx 0.18$ is obtained, if a scaling law for the Néel temperature and electron doping as the dominant mechanism of the T_N suppression are assumed: $T_N(\text{NdCuO}_4)=225$ K, $T_N(\text{Nd}_{1.91}\text{Ce}_{0.09}\text{CuO}_4)\approx 160$ K compared with $T_N(\text{PrBa}_2\text{Cu}_3\text{O}_6)=300$ K, $T_N(\text{PrBa}_2\text{Cu}_3\text{O}_7)=280-370$ K, and $T_N(\text{YBa}_2\text{Cu}_3\text{O}_6)=415$ K. This estimate is in accord with the specific-heat and susceptibility data of Hilscher *et al.* (Ref. 73) suggesting $z\approx 0.1$.
- ⁶⁰N. Kothekar, K.F. Quader, and D.W. Allender, *Phys. Rev. B* **51**, 5899 (1995).
- ⁶¹M. Guillaume, P. Allensbach, J. Mesot, B. Roesli, U. Staub, P. Fischer, and A. Furrer, *Z. Phys. B* **90**, 13 (1993).
- ⁶²W.A. Harrison, *Electronic Structure and Properties of Solids* (Freeman, San Francisco, 1980).
- ⁶³K.W. Becker, W. Brenig, and P. Fulde, *Z. Phys. B* **81**, 165 (1990).
- ⁶⁴N.M. Plakida, R. Hayn, and J.L. Richard, *Phys. Phys. B* **81**, 16 599 (1995).
- ⁶⁵L.F. Mattheiss and D.R. Hamann, *Phys. Rev. B* **40**, 2217 (1989).
- ⁶⁶K. Schwarz, C. Ambrosch-Draxl, and P. Blaha, *Phys. Rev. B* **42**, 2051 (1990).
- ⁶⁷S. Ramesh and M.S. Hedge, *Physica C* **230**, 135 (1994).
- ⁶⁸K. Nehrke, M. Pieper, and T. Wolf, *Phys. Rev. B* **53**, 229 (1996).
- ⁶⁹K. Takenaka, Y. Imanaka, K. Tamasaku, T. Ito, and S. Uchida, *Phys. Rev. B* **46**, 5833 (1992).
- ⁷⁰The experimentally observed conductivity peak near 0.2 – 0.3 eV is attributed in this model to a Drude peak shifted to finite frequencies due to the finite chain length $N\sim 20$. Neglecting clustering of defects, such typical chain lengths are expected considering vacancies at O(1) sites in $\text{YBa}_2\text{Cu}_3\text{O}_{6.95}$.
- ⁷¹In addition we note that ongoing from $n=1.5$ to $n=2$, there is only a small increase in the calculated total strength F_{tot} of the f -sum rule for the four-band dp model, where the calculated expectation value of the kinetic energy [bond order values (Eq. (7))] have been used (Refs. 74–77). The reflectivity data of Widder (Ref. 54) reveals a 14% reduction of the low-frequency oscillator strength centered near 0.2 eV for PBCO. Further theoretical investigations are necessary to determine the frequency and the size dependences of the optical conductivity in the present model.
- ⁷²M. Meinders, H. Eskes, and G. Sawatzky, *Phys. Rev. B* **48**, 3916 (1993).
- ⁷³G. Hilscher, E. Holland-Moritz, T. Holubar, H.-D. Jörnstarndt, V. Nekvasil, G. Schaudy, U. Walter, and G. Fillion, *Phys. Rev. B* **49**, 535 (1994).
- ⁷⁴S.R. Phillpot, A.R. Bishop, and B. Horovitz, *Phys. Rev. B* **40**, 1839 (1989).
- ⁷⁵D. Baeriswyl, J. Carmelo, and A. Luther, *Phys. Rev. B* **33**, 7247 (1986).
- ⁷⁶P.F. Maldague, *Phys. Rev. B* **16**, 2437 (1977).

- ⁷⁷C.A. Stafford and A.J. Millis, *Phys. Rev. B* **48**, 1409 (1993).
- ⁷⁸J. Hirsch, *Phys. Rev. Lett.* **53**, 2327 (1984).
- ⁷⁹Neutron scattering measurements of K. Kojima (see Ref. 30) unpublished 1996; compare also with the muon spin resonance (μ SR) data of Ref. 27 yielding $T_N \sim 4.15 - 6$ K.
- ⁸⁰M. Ogata and H. Shiba, *Phys. Rev. B* **41**, 2326 (1990).
- ⁸¹K. Hallberg, *Phys. Rev. B* **52**, R9827 (1995).
- ⁸²M. Meinders, Ph.D. thesis, Rijksuniversiteit Groningen 1994, p. 86.
- ⁸³J. Callaway, D. Chen, D. Kanhere, and Q. Li, *Phys. Rev. B* **42**, 465 (1990).
- ⁸⁴F. Assaad and D. Würtz, *Phys. Rev. B* **44**, 2681 (1991).
- ⁸⁵S. Haas, E. Dagotto, A. Nazarenko, and J. Riera, *Phys. Rev. Lett.* **51**, 5989 (1995).
- ⁸⁶E. Dagotto, *Rev. Mod. Phys.* **66**, 763 (1994).
- ⁸⁷J. Malek, S.-L. Drechsler, and G. Paasch (unpublished).
- ⁸⁸P. Wochner, E. Isaacs, S. Moss, P. Zschack, J. Giapintzakis, and D. Ginsberg (unpublished).
- ⁸⁹S. Inagaki and H. Fukuyama, *J. Phys. Soc. Jpn.* **52**, 3620 (1983).
- ⁹⁰N. Katoh and M. Imada, *J. Phys. Soc. Jpn.* **63**, 4529 (1994).
- ⁹¹H. Eskes and A. Oles, *Phys. Rev. Lett.* **73**, 1279 (1994).